Bulletin of the Seismological Society of America, Vol. 104, No. 5, pp. 2399–2411, October 2014, doi: 10.1785/0120140084

The Destiny of a Clast within a Molten Pseudotachylyte Vein

by Andrea Bizzarri

Abstract Pseudotachylytes are important markers that can indicate the thermal state during a coseismic slip failure and provide indirect information about the level of stress and sliding velocities attained during that time window. On the other hand, survivor, fragmented clasts embedded in the quenched material are also very important, in that they provide information about the energy spent to create new fracture surfaces. In this paper, I study the temperature evolution of clasts subjected to the heat dissipated by a just-formed, molten pseudotachylyte (PT) vein. In particular, I find the analytical solutions for the temperature evolution within the PT vein, the surrounding, undamaged host rock, and inside a clast. According to the proposed model, the numerical results show that the clasts tend to preferentially melt in the inner part of the PT vein (i.e., they are completely assimilated by the PT). In contrast, some clasts can survive far from the PT vein center. My solutions, although based upon a simplified model, can provide a theoretical framework to predict the maximum size of the survived clasts at a given distance from the PT center. The distribution of these survivor clasts follows a power-law relation in terms of their radius, and its features generally agree with field and laboratory observations.

Introduction

There is no doubt that the problem of the energy balance for an earthquake event is one of the central issues in the physics of the earthquake source (e.g., Dahlen, 1977; Husseini, 1977; Rudnicki and Freund, 1981; Kostrov and Das, 1988; Rivera and Kanamori, 2005; Cocco *et al.*, 2007; Bizzarri, 2013). On the other hand, pseudotachylyte (PT; glassy-like, aphanitic, black-colored rocks; Shand, 1916) is the unique fault rock that is known to be created during the coseismic time window (i.e., at seismic slip rates [∼1–10 m/s or more] when the major stress release occurs on a fault). As a consequence, the presence of PT is of extraordinary importance, because it preserves direct evidence of the dynamic, energy-dissipating chemical and physical mechanisms that occur during earthquake ruptures (Sibson, 1975; Cowan, 1999). In more detail, PTs are interpreted as markers of the heating processes that occur during the fast sliding on the fault (McKenzie and Brune, 1972; Sibson, 1975; Spray, 1993, 1995; Ikesawa *et al.*, 2003; Andersen and Austrheim, 2006; Sibson and Toy, 2006; Lin, 2008). Although PTs rarely can be preserved or even recognized (see Sibson and Toy, 2006; Kirkpatrick *et al.*, 2009; and Kirkpatrick and Rowe, 2013, for detailed discussion), they are regarded as markers of a melting process (Philpotts, 1964; Sibson, 1975; Maddock, 1983; Spray, 1987; Lin, 1991; Kirkpatrick *et al.*, 2012). Indeed, localized melting at asperity contacts is predicted theoretically (Jeffreys, 1942; McKenzie and Brune, 1972; Rempel and Rice, 2006; Bizzarri, 2009), and a plethora of theoretical and numerical models indicates that melting temperatures for rock-forming minerals can be easily exceeded during seismic sliding (among others, Fialko and Khazan, 2005; Bizzarri and Cocco, 2006b; Nielsen *et al.*, 2008; Bizzarri, 2011). Indeed, evidence of melting on major faults during great earthquakes does exist; examples include the Outer Hebrides thrust, Scotland (Sibson, 1975), the Priestley fault, Antarctica (Storti *et al.*, 2001), and the Pasagshak Point thrust subduction décollement, Alaska (Rowe *et al.*, 2005).

On the other hand, Pittarello *et al.* (2008) estimate the surface energy (i.e., the energy required to create new fracture surfaces) by analyzing the density of microcracks inside the clasts entrapped in a PT vein and in the fault wall rock. A clast is a rock fragment or a cracked grain that results from the breakdown of larger rocks; an example can be found in figure 3b of Pittarello *et al.* (2008). Indeed, the clast itself can be internally cracked (Keulen *et al.*, 2007) due to different mechanisms, such as thermal fracturing (Ohtomo and Shimamoto, 1994), abrasive wear (Rabinowicz, 1965), and process zone microfracturing (Reches and Dewers, 2005).

The presence of survivor clasts (i.e., nonmolten clasts), due to fragmentation, inside a PT vein can be of great importance in the attempt to formulate the energy balance equation of an earthquake. Several studies have attempted to retrieve the magnitude of dynamic shear resistance from the clast content in the PT veins (e.g., Spray, 1992; Ujiie *et al.*, 2007; Kirkpatrick *et al.*, 2012).

In this paper, I consider the problem of the survival of a clast embedded into a just-formed (new) PT vein. I will

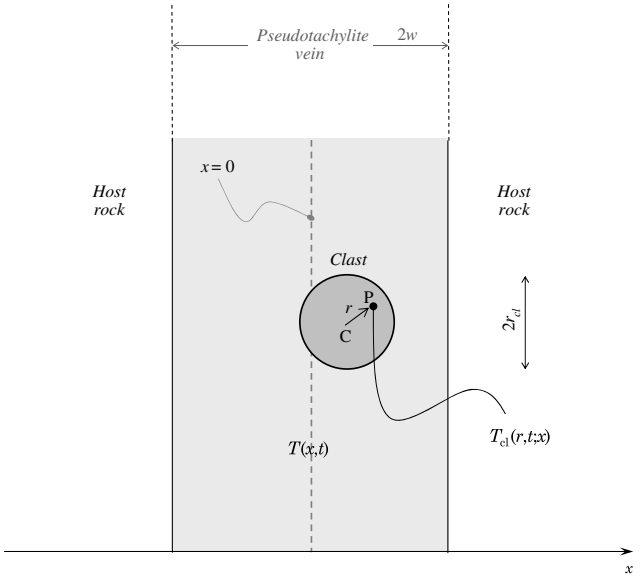

Figure 1. A schematic view of the system considered in the paper: a homogeneous pseudotachylyte (PT) vein of constant thickness $2w$ is embedded in an infinite surrounding host rock that also has uniform material properties. The distance of a point P in the clast from its center C is denoted by $r(0 \le r \le r_{cl})$, whereas the distance of C from the center of the vein is indicated with $x(-w \le x \le w)$. The figure shows a cross section of the PT vein, which extends in the direction perpendicular to the reader.

explore the conditions controlling its survival, expressed in terms of its position with respect to the vein center and its dimensions. The theoretical framework proposed here, as with every theoretical model of a natural phenomenon, is based upon some assumptions and simplifications, which are scrutinized in the Discussion section. Nevertheless, the proposed model is, to date, the first framework to predict the evolution (fate) of a clast embedded in a PT vein and to explain the power-law distribution of the nonmolten (surviving) clasts.

The problem of the cooling of a PT vein is solved analytically in a closed form in the Temperature within the Pseudotachylyte Vein section, whereas in the Temperature Inside a Single Clast section, I found an analytical solution for the temperature inside a spherical clast. The Numerical Results, Frequency Distribution of the Surviving Clasts, and Sensitivity Tests sections are devoted to the discussion of the numerical results, based on some realistic scenarios. The Conclusive Remarks section summarizes the conclusions of the present work.

Temperature within the Pseudotachylyte Vein

In this paper, I consider a PT vein with width of $2w$ embedded in an infinite, homogeneous medium, as depicted in Figure 1. For simplicity, I deliberately neglect any possible corrugation or geometrical irregularity in the shape of the vein, although I know that in some cases the molten material can be ejected from the fault core and can penetrate into the surrounding damage zone (see, for example, fig. 3a of Pittarello *et al.*, 2008, and fig. 1a of Kirkpatrick and Rowe, 2013). The initial temperature of such a system is $T_0(x) \equiv T(x,0)$, in which $x \in]-\infty, +\infty[$. (The complete list of the symbols used in this paper is reported in Table 1.) I assume here that there is no any heat source internal to the system (due, for instance, to viscous shearing or frictional heat); indeed, I am interested in the behavior of the PT vein instead of the physical processes leading to its creation, which have been considered elsewhere (e.g., Bizzarri, 2011, and references cited therein).

Table 1
Representative Parameters Used in This Paper

Parameter	Description	Value
w	Half-thickness of the pseudotachylyte (PT) vein	2.95×10^{-3} m
r_{cl}	Radius of the clast	1×10^{-3} m
x	Distance from the center of the PT vein	n/a
t	Time	n/a
$T(x,t)$	Temperature field in the medium	n/a
$T_0(x) \equiv T(x,0)$	Initial temperature profile in the medium	See equation (2).
T_{melt}	Effective melting temperature of the PT vein	1450°C
$T_{melt_{cl}}$	Melting temperature of the clast	1200°C
T_{hr}	Temperature of the host rock	250°C
r	Distance from the center of the clast	$\le r_{cl}$
$T_{cl}(r,t;x)$	Temperature field inside the clast	n/a
T_{cl_0}	Initial temperature of the clast	250°C
χ	Thermal diffusivity	7.2×10^{-7} m^2/s
χ_{cl}	Thermal diffusivity of clast	1.75×10^{-6} m^2/s

In this case, the temperature $T(x,t)$ at time t and at a distance x from the center of the PT vein is expressed as the solution of the 1D Fourier's heat conduction equation ($\frac{\partial}{\partial t}T = \chi \frac{\partial^2}{\partial x^2}T$), which reads as

$$T(x,t) = \frac{1}{2\sqrt{\pi\kappa t}} \int_{-\infty}^{+\infty} T_0(x') e^{-\frac{(x-x')^2}{4\chi t}} dx' \qquad (1)$$

(Carslaw and Jaeger, 1959), in which χ is the thermal diffusivity ($\chi = \kappa/\rho C_p$, wherein κ is the thermal conductivity, ρ the cubic mass density of the material, and C_p its specific heat at constant pressure). χ might be spatially heterogeneous across the PT vein and across the host rock, depending on mineral composition; here I assume an average value for the whole space.

Let us assume that the initial temperature profile of the PT vein simply is

$$T_0(x) = \begin{cases} T_{melt}, & x \in [-w, w] \\ T_{hr}, & \text{elsewhere} \end{cases}, \qquad (2)$$

in which T_{melt} is the effective melting temperature within the PT vein and T_{hr} is the initial (reference) temperature of the undamaged host rock. The condition expressed by equation (2) states that the PT vein has just been formed, because its initial temperature is T_{melt} and it begins cooling at $t = 0$. Of course, the boxcar function represented by equation (2) is a simplification of the initial conditions for the PT vein temperature. One can alternatively assume other analytical functions, even smoothed, such as the Gaussian or other arbitrary formulations. Another possibility would be to use the steady state solution proposed by Nielsen *et al.* (2008; see for instance their figs. 4a and b), but I actually do not know if the applicability of a steady state condition is appropriate to the initial time; and, more importantly, I would add another free (and unknown) parameter into the model (the steady state sliding speed). In this paper, I conservatively assume the most simple, and plausible, initial condition, as stated by equation (2), allowing for the possibility that future work will give us sufficient constraints to consider more complex scenarios.

Once the function $T_0(x)$ is given, equation (1) can be evaluated; in the case of equation (2), simple algebra shows that one can obtain a closed-form analytical solution:

$$T(x,t) = \frac{1}{2}\left\{T_{melt}\left[\mathrm{erf}\left(\frac{w+x}{2\sqrt{\chi t}}\right) + \mathrm{erf}\left(\frac{w-x}{2\sqrt{\chi t}}\right)\right] + T_{hr}\left[\mathrm{erfc}\left(\frac{w-x}{2\sqrt{\chi t}}\right) + \mathrm{erfc}\left(\frac{w+x}{2\sqrt{\chi t}}\right)\right]\right\}, \quad (3)$$

in which $\mathrm{erf}(\cdot)$ is the error function ($\mathrm{erf}(z) \underset{df}{=} \frac{2}{\sqrt{\pi}}\int_0^z e^{-\xi^2} d\xi$) and $\mathrm{erfc}(\cdot)$ is its complementary function ($\mathrm{erfc}(\cdot) \underset{df}{=} 1 - \mathrm{erf}(\cdot)$). There is no need to overemphasize that this solution differs from previous ones in which an internal heat source was included in the model (e.g., Fialko, 2004; Bizzarri and Cocco, 2006a). In the center of the PT vein,

$$T(0,t) = T_{melt}\mathrm{erf}\left(\frac{w}{2\sqrt{\chi t}}\right) + T_{hr}\mathrm{erfc}\left(\frac{w}{2\sqrt{\chi t}}\right); \quad (4)$$

and, at the borders of the PT vein,

$$T(\pm w,t) = T_{melt}\mathrm{erf}\left(\frac{w}{\sqrt{\chi t}}\right) + T_{hr}\mathrm{erfc}\left(\frac{w}{\sqrt{\chi t}}\right). \quad (5)$$

From equations (4) and (5), $\lim_{t\to+\infty} T(0,t) = \lim_{t\to+\infty} T(\pm w,t) = T_{hr}$, which physically states that the whole system asymptotically regains its reference thermal state through time.

Temperature inside a Single Clast

Now, I consider a single spherical clast (of radius r_{cl}) with homogeneous properties, which is inserted at $t = 0$ in the PT vein (Fig. 1). Because the volume of a single clast V_{cl} is negligible with respect to the whole volume of the PT vein V, I can safely assume that the temperature evolution of the PT vein is not perturbed by the presence of the clast, so the solution in equation (3) is still valid. I emphasize here that the condition $V_{cl} \ll V$ does not absolutely imply $r_{cl} \ll 2w$; indeed, the PT vein has dimensions along the depth and along the strike directions that are very large compared to its size ($2w$). Consequently, the total volume of the PT vein is basically controlled by these dimensions, not by $2w$.

In general, the total volume of the clasts may also have an impact on the vein cooling; this translates into the fact that the PT vein temperature expressed by equation (3) should be regarded as an upper bound of the actual PT temperature. Nevertheless, many studies (e.g., Di Toro *et al.*, 2005; Kirkpatrick *et al.*, 2012) show that the final clast content is relatively low (on the order of 20% or less), so that the perturbation due to the clast volume is small.

Although clasts can have shape different than a sphere, I made this assumption in the interest of simplicity and to obtain an analytical solution to this problem (see the Discussion section). In particular, I wish to know the temperature inside the whole clast, the increase of which is caused by the heat exchange through time due to heating by the hotter PT vein. Moreover, I assume that the clasts that were already formed within the PT vein were formed through fracturing processes prior to melting and formation of the PT vein fill, such as wear, fragmentation, and other comminution processes (e.g., Sibson, 2003). Therefore, I neglect the problem of the clast generation during a cosesimic slip event, as my focus is the fate of the clasts rather than their formation.

I assume that the initial temperature of the clast (T_{cl_0}) is uniform inside its entire volume. Letting the center of the clast be at a distance x from the PT vein center (Fig. 1), its surface temperature (for $r = r_{cl}$) equals the temperature $T(x,t)$ expressed by equation (3). In the special case in which a clast can be geometrically viewed as a protrusion of the host rock, its initial surface temperature is still expressed by equation (3), which accounts for the temperature with and without the PT vein.

At time $t > 0$ and at a distance $0 \le r < r_{cl}$ from its center (namely, in the point P reported in Fig. 1), the temperature $T_{cl}(r,t;x)$ of the clast is expressed as (Carslaw and Jaeger, 1959; their chapter 9, equation 3)

$$T_{cl}(r,t;x) = \frac{2}{r_{cl}r}\sum_{m=1}^{+\infty} e^{-\frac{\chi_{cl}m^2\pi^2 t}{r_{cl}^2}} \times \sin\left(\frac{m\pi r}{r_{cl}}\right)(I_1 - \chi_{cl}m\pi(-1)^m I_2(t;x)). \quad (6)$$

In equation (6) χ_{cl} is the thermal diffusivity of the clast and

$$I_1 \equiv \int_0^{r_{cl}} T_{cl_0} r' \sin\left(\frac{m\pi r'}{r_{cl}}\right) dr' \quad (7)$$

and

$$I_2(t;x)\equiv\int_0^t e^{\frac{\chi_{\rm cl}m^2\pi^2t'}{r_{\rm cl}^2}}T(x,t')dt'. \quad (8)$$

(Readers can refer to chapter 9 of Carslaw and Jaeger, 1959, for additional analytical details.) Equations (6)–(8) assume that the surface temperature of the spherical clast is spatially uniform and equal to $T(x,t)$; I discuss this issue in detail in Appendix A.

Once the melting temperature of the clast $T_{\rm melt_{cl}}$ is exceeded, the clast starts to melt, and therefore one deals with a Stefan problem (e.g., Nielsen *et al.*, 2008; Bizzarri, 2011, and references cited therein), which controls the kinetics of the solid/melt boundaries of the melting clast. In such a case, I would have to consider the latent heat of melting of the clast. The incorporation of such a latent heat into the model will have no effect on the temperature of the PT vein, but it would tend to buffer the temperature of the partially melting clast. Here, when a clast starts to melt, I ignore the latent heat of melting of the clast. Considering that the integral in equation (7) simply gives $I_1=-\frac{(-1)^m r_{\rm cl}^2 T_{\rm cl_0}}{m\pi}$, I rewrite equation (6) as

$$T_{\rm cl}(r,t;x)=-\frac{2}{r_{\rm cl}r\pi}\sum_{m=1}^{+\infty}\frac{(-1)^m}{m}e^{-\frac{\chi_{\rm cl}m^2\pi^2t}{r_{\rm cl}^2}}\sin\left(\frac{m\pi r}{r_{\rm cl}}\right)(r_{\rm cl}^2T_{\rm cl_0}+\chi_{\rm cl}m^2\pi^2I_2(t;x)). \quad (9)$$

The integral I_2 in equations (6) and (9), defined in equation (8), has to be solved numerically. To this goal, it is computationally convenient to rearrange equation (9) as

$$T_{\rm cl}(r,t;x)=-\frac{2}{r_{\rm cl}r\pi}\sum_{m=1}^{+\infty}\frac{(-1)^m}{m}\sin\left(\frac{m\pi r}{r_{\rm cl}}\right)(r_{\rm cl}^2T_{\rm cl_0}e^{-\frac{\chi_{\rm cl}m^2\pi^2t}{r_{\rm cl}^2}}+\chi_{\rm cl}m^2\pi^2I_3(t;x)), \quad (10)$$

in which

$$I_3(t;x)\equiv\int_0^t e^{\frac{\chi_{\rm cl}m^2\pi^2(t'-t)}{r_{\rm cl}^2}}T(x,t')dt'. \quad (11)$$

In order to compute I_3, I adopt a general-purpose integrator (modified from Piessens *et al.*, 1983) that uses a globally adaptive scheme to reduce the absolute error. It subdivides the interval of integration (in my case $[0,t]$) and uses a $(2k+1)$-point Gauss-Kronrod quadrature rule to estimate the integral over each subinterval. The error for each subinterval is estimated by comparison with the k-point Gauss quadrature rule. The subinterval with the largest estimated error is then bisected, and the same procedure is applied to both halves. The bisection process is continued until the error criterion is satisfied, round-off error is detected, the subintervals become too small, or the maximum number of subintervals allowed is reached.

Because $\sum_{m=1}^{+\infty}\frac{(-1)^m}{m}\sin(\frac{m\pi r}{r_{\rm cl}})=-\frac{\pi r}{2r_{\rm cl}}$, equation (10) can be rewritten in the following form:

$$T_{\rm cl}(r,t;x)=\frac{\sum_{m=1}^{+\infty}t_m(r)(T_{\rm cl_0}e^{-\frac{\chi_{\rm cl}m^2\pi^2t}{r_{\rm cl}^2}}+\frac{\chi_{\rm cl}m^2\pi^2}{r_{\rm cl}^2}I_3(t;x))}{\sum_{m=1}^{+\infty}t_m(r)}, \quad (12)$$

in which

$$t_m(r)\equiv\frac{(-1)^m}{m}\sin\left(\frac{m\pi r}{r_{\rm cl}}\right). \quad (13)$$

I remark here that the numerical treatment of equation (12) is more accurate than that of equation (10), especially for small values of r and t. First, from equation (12), it is trivial to verify that $T_{\rm cl}(r,0;x)=T_{\rm cl_0}$ for any r and x, as expected. Moreover, for an arbitrarily large value of $m_{\rm max}$, the numerical estimate

$$\hat{T}_{\rm cl}(r,t;x)=\frac{\sum_{m=1}^{m_{\rm max}}t_m(r)(T_{\rm cl_0}e^{-\frac{\chi_{\rm cl}m^2\pi^2t}{r_{\rm cl}^2}}+\frac{\chi_{\rm cl}m^2\pi^2}{r_{\rm cl}^2}I_3(t;x))}{\sum_{m=1}^{m_{\rm max}}t_m(r)} \quad (14)$$

will converge to the exact value $T_{\rm cl}(r,t;x)$ of equation (12). (Equation 14 is the truncation of the summation in equation (12) up to $m_{\rm max}$.) In particular, in the center of the clast (i.e., for $r=0$), by recalling that $\lim_{r\to0}\frac{1}{r}\sin(\frac{m\pi r}{r_{\rm cl}})=\frac{m\pi}{r_{\rm cl}}$, it is trivial to demonstrate that equation (14) simply reduces to

$$\hat{T}_{\rm cl}(0,t;x)=\frac{\sum_{m=1}^{m_{\rm max}}(-1)^m(T_{\rm cl_0}e^{-\frac{\chi_{\rm cl}m^2\pi^2t}{r_{\rm cl}^2}}+\frac{\chi_{\rm cl}m^2\pi^2}{r_{\rm cl}^2}I_3(t;x))}{\frac{1}{2}((-1)^{m_{\rm max}}-1)}, \quad (15)$$

which does not diverge if $m_{\rm max}$ is odd.

Numerical Results

In this paper, I assume that the PT vein is 5.9 mm wide; this is the average value found by Pittarello *et al.* (2008) based on measurements from the high-resolution digital photomosaics of the planar segment from the Gole Larghe fault, Adamello, Italy. This target site is an example of one of the most well-studied PT-bearing fault zones; however, because the clast size distribution is affected by cataclasis (Magloughlin, 1992; Di Toro *et al.*, 2005, and references cited therein; Fialko and Khazan, 2005), I do not expect my current results on the clast size distribution (see the Frequency Distribution of the Surviving Clasts section) can be applied literally to that case. The other parameters of the model are tabulated in Table 1, again in agreement with the data from the Gole Larghe fault; in the Sensitivity Tests section, I will also explore different configurations to generalize my results.

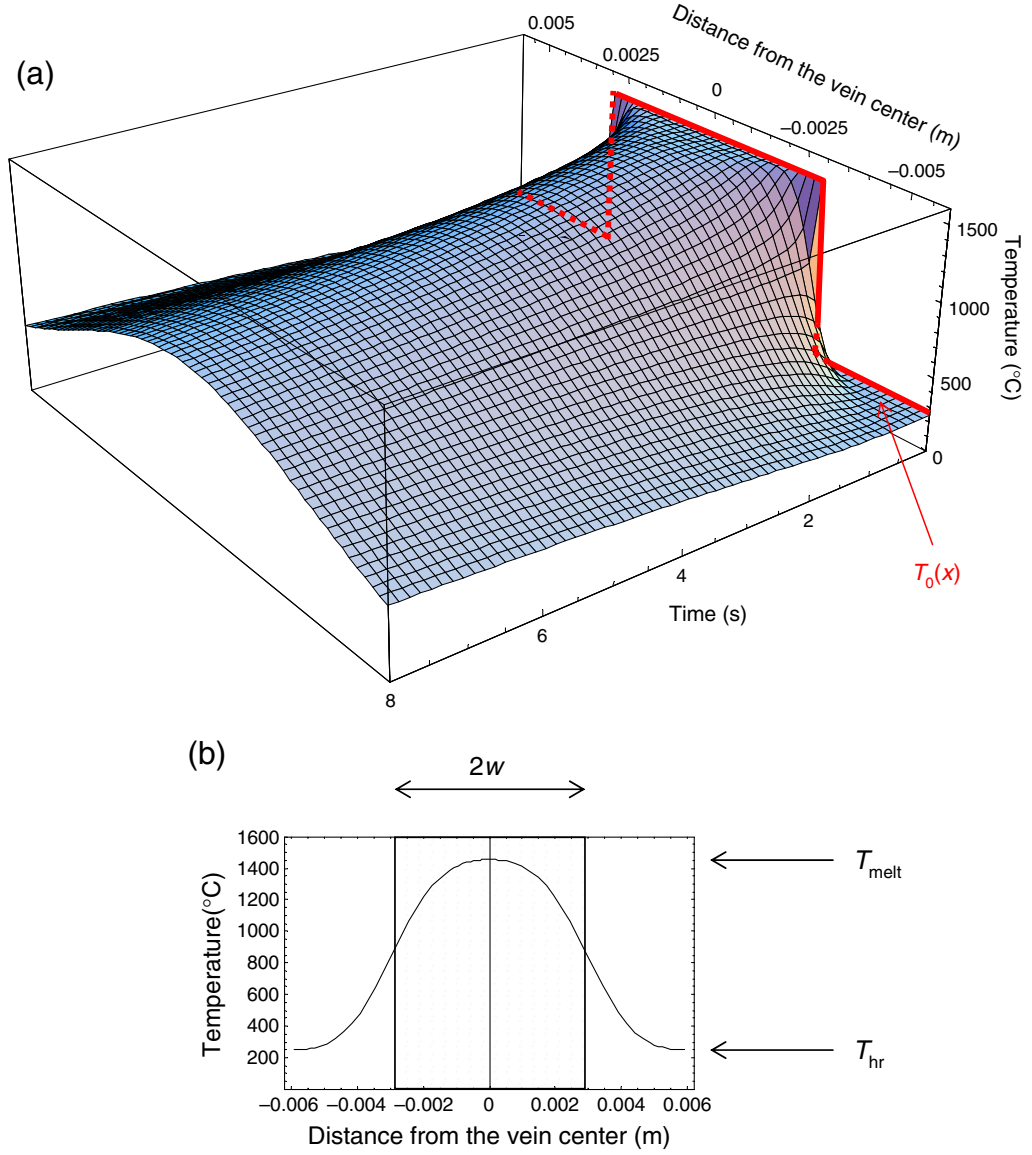

Figure 2. (a) Spatiotemporal evolution of the temperature in the medium for the parameters listed in Table 1. The initial condition $T_0(x)$ (thick line) is specified in equation (2), and the values of T are given by equation (3). (b) The temperature profile across the medium is calculated at $t = 1$ s in the same conditions as in panel (a). The rectangle indicates the location of the PT vein. The color version of this figure is available only in the electronic edition.

The melting temperature of the PT vein (initial PT temperature) was chosen according to the observation of Nestola *et al.* (2010), who established that the molten PT layer experiences temperature equal to 1450°C due to the presence of the dmisteinbergite. On the other hand, I consider clasts made by plagioclase, for which the melting temperature is 1200°C. The initial temperature of the PT vein exceeds that of the clast because it fails in superheating conditions. Finally, the temperature of the wall rock away from the PT vein (T_{hr} in equation 2) has been set according to the estimates from the mineral assemblage far from the PT (Di Toro and Pennacchioni, 2004); $T_{hr} = 250$°C.

Figure 2a shows the spatiotemporal distribution of the temperature of the PT vein for the typical parameters listed in Table 1, as given by the closed-form analytical solution in equation (3). After $t = 0$ the vein starts to cool, and concurrently the host rock warms.

Figure 3 depicts the time evolution of T within (thick lines) and outside (thin lines) the PT vein for the same parameters. It is clear also from Figure 3a that the PT vein cools, while the host warms up. At around $t = 3$ s, the boundaries of the PT vein (i.e., $|x| = 2.95$ mm) tend to reach an intermediate equilibrium temperature, equal to $(T_{melt} + T_{hr})/2$. Afterward, the whole system cools, and it reaches the final temperature of the host rock (i.e., the ambient, reference temperature T_{hr}; see Fig. 3b). This outcome is reasonable, in that the heat lost by the PT vein initially warms the host rocks and finally dissipates, so that the whole system regains its

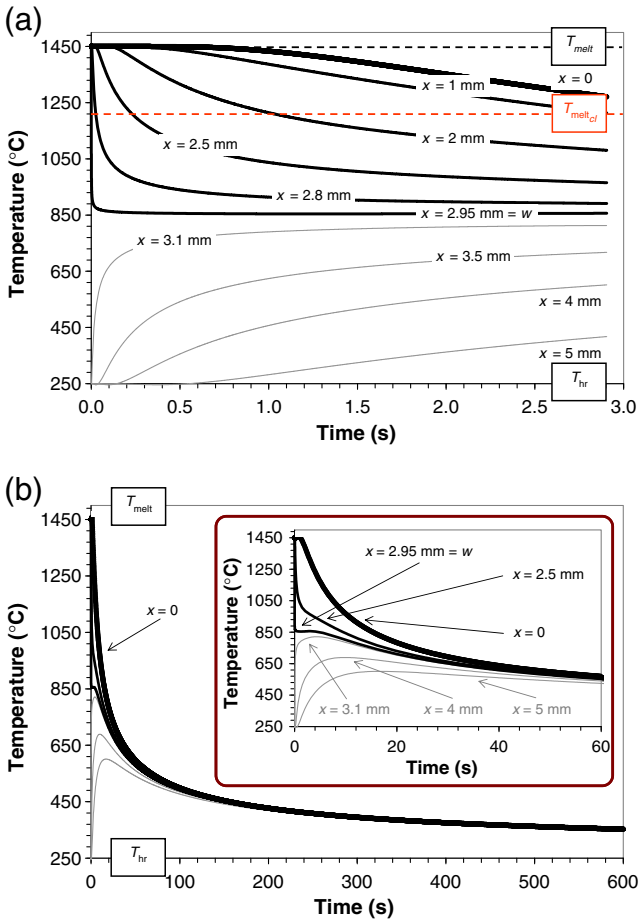

Figure 3. Time evolution of the temperature in the medium at different distances x from the center of the PT vein (indicated near each curve). Thick and thin lines pertain to locations within and outside the PT vein, respectively. The very thick line identifies the temperature in the center of the PT vein (as expressed by equation 4). Relevant temperatures are also indicated. (a) Time window is up to 3 s. (b) Time window is up to 10 min, with the inset panel reporting times up to 1 min. The color version of this figure is available only in the electronic edition.

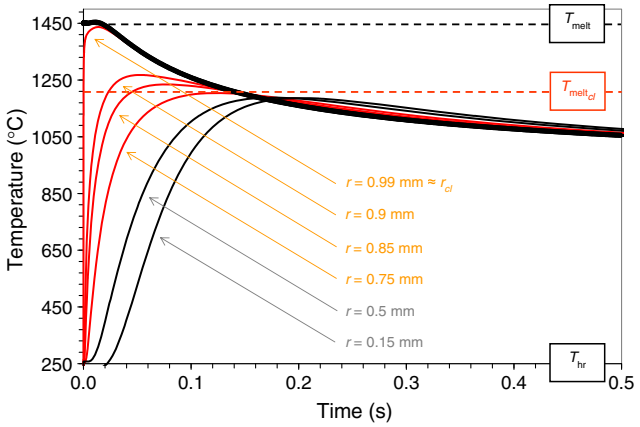

Figure 4. Temperature evolution inside a single, isolated clast located at a distance $x = 2.6$ mm from the PT vein center. The different distances r from the center of the clast at which T_{cl} is computed are indicated near each curve. The thick line indicates the temperature evolution of the PT vein, namely T computed from equation (3). T_{cl} is computed from equation (14). Relevant temperatures are also indicated. The color version of this figure is available only in the electronic edition.

reference thermal state (T_{hr}). The asymptotic limit depicted in Figure 3b confirms the theoretical predictions discussed at the end of the Temperature within the Pseudotachylyte Vein section.

In Figure 4, I plot the temperature inside a single, isolated clast T_{cl}, as given by equation (14). It refers to a clast centered at a distance $x = 2.6$ mm from the PT vein center. In this example, I have deliberately chosen a clast with an initial large radius ($r_{cl} \sim w/3$) to see the different temperature profiles depending on many distances from the center of the clast. Until the final radius of the surviving clast is reduced to 0.35 mm, a part of the clast is out of the PT vein. The thick line indicates the ambient temperature, that is, the temperature T of the PT vein (as given by equation 3). The various lines refer to different positions r with respect to the center of the clast. Because of the heat transferred from the PT vein, T_{cl} increases starting from $t = 0$, with a rate that is inversely proportional to r. For inner points (i.e., for smaller r), T_{cl} increases more slowly than for points close to the external surface of the clast (i.e., for larger r). This behavior is reasonable, because as long as r approaches r_{cl}, T_{cl} asymptotically collapses to T.

After 0.2 s T_{cl} roughly equals T, indicating that the system has reached its thermal equilibrium; for larger times the two temperatures evolve identically and asymptotically tend to the final temperature (recall Fig. 3b). The most important outcome of Figure 4 is that for $r \geq 0.75$ mm the clast start to melt. At this particular distance x, and for the adopted parameters, my results indicate that the maximum size of a survivor (i.e., not molten) clast fails in the range between 0.5 and 0.75 mm.

For a given set of thermal parameters and size of the PT vein, the maximum size (radius) of a survivor clast depends on the distance x of the clast center from the PT vein center. To analyze such a dependence, I report in Figure 5 a phase diagram summarizing the behavior of the clasts as a function of the two distances x and r. For each position x, I first compute the temperature in the center of the clast (i.e., for $r = 0$). If this temperature exceeds the melting temperature, this implies that the whole clast melts and it is completely assimilated into the PT vein. This situation is reported by a full circle. If the temperature at $r = 0$ does not exceed the melting temperature of the clast $T_{melt_{cl}}$, then I consider $r > 0$ and identify (again for the target position x) the maximum value of r for which the temperature of the clast T_{cl} is below $T_{melt_{cl}}$. I repeat this computation for all possible distances x. This computation makes it possible to consider not only the two end members (molten or nonmolten clasts, which clearly emerge from the distinction between open and full circles in Fig. 5), but also the process of partial melting. For example,

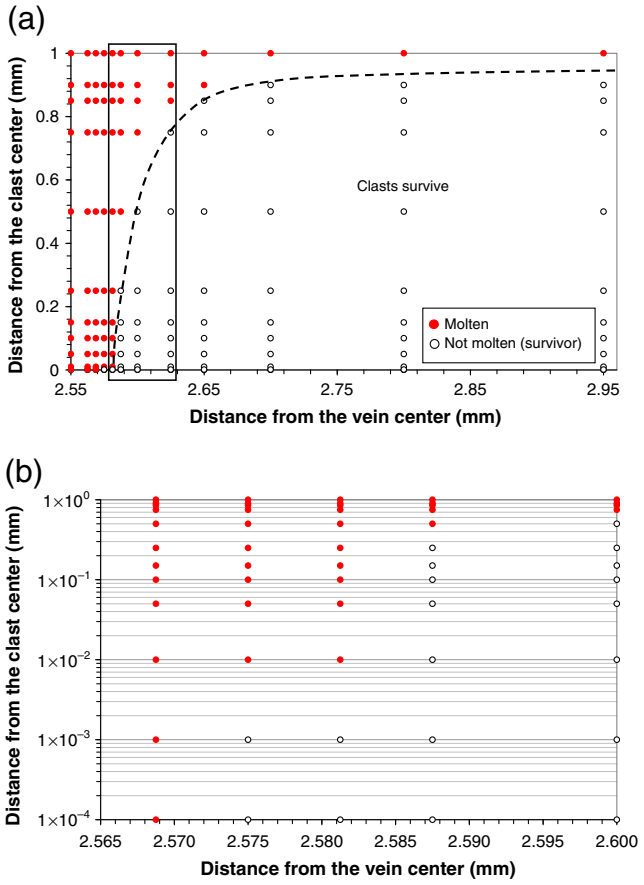

Figure 5. Phase diagram reporting the maximum size of the surviving clasts at a given distance x from the PT vein center. Filled circles denote molten clasts (i.e., the clasts that are completely destroyed and incorporated into the PT vein). Empty circles denote the survivor clasts. In (a), the dashed curve separates the phase space where the clasts survive from that where they melt completely. (b) The enlarged view of the region marked by the rectangle in panel (a) shows the clasts in a semilogarithmic plot. The color version of this figure is available only in the electronic edition.

if one considers the distance $x = 2.6$ mm, a clast with an initial radius $r_{\mathrm{cl}} = 1$ mm partially melts and survives when $r_{\mathrm{cl}} = 0.5$ mm. On the other hand, if a clast has an initial radius $r_{\mathrm{cl}} = 0.15$ mm, it survives completely at the target distance x.

The phase portrait in Figure 5 collects nearly 200 numerical simulations. For the parameters assumed here, for $x \leq 2.56875$ mm all clasts melt and are completely assimilated by the PT vein; I will critically discuss this result in the Discussion section. Similarly, no clasts with a radius of 1 mm survive.

In general, for a given value of x (i.e., for a fixed value in the abscissa), the larger survivor clast is that having the largest r associated with an empty circle. (Analogously, for a given r [i.e., for a fixed value in the ordinate], the minimum distance at which a clast with that radius survives is the first value [moving to the left] with an empty circle.) In Figure 5a, the dashed line denotes the separation between the survivor clasts and the molten ones. Figure 5b depicts an enlarged view of the rectangle in Figure 5a, which pertains to the transition between molten and nonmolten clasts.

The boundary between the molten and survivor clasts reported in Figure 5 depends on the adopted parameters (Table 1); in the Sensitivity Tests section I scrutinize the behavior of the system for other configurations. In general, it is difficult to perform quantitative, exact comparisons with cases reported in the literature. For an example, Pittarello *et al.* (2008) found that no clasts survive with radius greater than roughly 0.01 mm at Gole Large fault, whereas Chester *et al.* (2005) found a maximum radius roughly of 0.1 mm at Punchbowl fault. More explicit comparison against observation can be done when one considers the statistical distribution of the surviving clasts, which is the topic of the next section.

Frequency Distribution of the Surviving Clasts

The distribution of the (surviving) clasts has received great attention in the literature, not only in the framework of the PT veins, but also in different contexts (e.g., Sammis and King, 2007; Pittarello and Koeberl, 2013). Notably, Ray (1999) observes that the grain-size reduction due to cataclasis along fault interfaces (after the onset of slip, the intact wall rocks are crushed and generate rock fragments, with progressively reducing size) follows a power-law (fractal, and thus scale-invariant) size–frequency distribution. In the context of the PT vein, Shimamoto and Nagahama (1992) and Chester *et al.* (2005; see their fig. 3b) reported that surviving clasts obey a power-law size distribution. Considering exhumed samples from the Gole Larghe fault, Italy, Pittarello *et al.* (2008; see their fig. 4) found a power-law distribution for the surviving clasts, over roughly two orders of magnitudes. Kirkpatrick and Rowe (2013; their fig. 7d) also found a power-law distribution with a constant slope over a small range of radii.

My current model can provide, as a side result, the opportunity to study the distribution of the surviving clasts. To determine the number of surviving clasts, I consider all possible distances x_i from the center of the PT vein. Then I compute the temperature of a single clast centered at each x_i; the maximum radius r_{s_i} at which the temperature of the clast is below the melting temperature $T_{\mathrm{melt_{cl}}}$. The number of the surviving clasts, $N_i \equiv N(r = r_{s_i})$, having a given radius r_{s_i} is expressed as

$$N_i = 2\left[\mathrm{int}\left(\frac{w - (x_i + r_{s_i})}{2r_{s_i}}\right) + 1\right]. \qquad (16)$$

In equation (16), the subscript i indicates the discrete values of the distance x from the center of the PT vein and the values of the maximum radius of the survivor clast r_s at that distance (see Fig. 5). The factor 2 accounts for the symmetry of the problem with respect to $x = 0$. Moreover, equation (16) assumes that the clasts cannot interpenetrate (and therefore

the available space, for $0 \le x \le w$, for clasts of radius r_{s_i} is $w - (x_i + r_{s_i})$; the same is true of $-w \le x \le 0$). Finally, I exclude the clasts that are not completely within the total size of the PT vein (namely, I put $N_i = 0$ when $w - (x_i + r_{s_i}) < 0$). It is important to note that because I deal with a single clast at once, I do not consider any specific parental (i.e., initial) clast distribution.

The cumulative number N_i^{cum} of clasts with $r \ge r_{s_i}$ simply is

$$N_i^{\text{cum}} = N_i + N_{i-1}^{\text{cum}}. \tag{17}$$

The resulting distribution N^{cum} versus r_s is reported in a log–log scale in Figure 6, from which emerges a power-law behavior of the type

$$N^{\text{cum}} = C\, r_s^{-D}. \tag{18}$$

I note a smaller (negative) slope for finer clasts, in agreement with previous studies (e.g., Pittarello *et al.*, 2008); this reflects in a different exponent D (I have $C = 0.98$ and $D = 0.90$ for $r < 0.1$ mm and $C = 0.24$ and $D = 1.5$ for $r > 0.1$ mm). Data from postmelting clast products from the Sawar–Junia sector, India, analyzed by Ray (2004; his table 1b) indicate a clear distinction between small and large clasts in that a different power-law exponent describes the two ranges. In particular, he found that the power-law exponent is larger for larger clasts radii. My results are in agreement with his findings, although an exact, direct comparison is difficult because his data include clasts of exceptionally large size (with radii up to 28 mm), which also implies a much larger PT vein thickness. Remarkably, I found that the threshold between small and large clasts (i.e., the critical value of radius at which the power-law exponent changes) has a direct proportionality with the PT vein thickness.

I also remark here that the exponents D that I retrieve can underestimate the true D, because in equation (16), and thus in equation (17), I account only for clasts with center at the same depth, although a denser distribution is possible if I account for contacting clasts which do not have centers aligned along the y axis.

Interestingly, Tsutsumi (1999) found that for experimentally generated PT, the clast size distribution still follows a power-law behavior, which is slightly modified with respect to equation (18). Namely,

$$N^{\text{cum}} = C'\left(1 + \frac{r_s}{E'}\right)^{-D'}, \tag{19}$$

in which E' is a constant that depends on the material.

Sensitivity Tests

The survival of a clast, at a given distance from the PT vein center depends on the chosen parameters. In order to better explore the behavior of the system, I first consider a model in which the initial radius is $r_{\text{cl}} = 2.5$ mm. In Figure 7, I report the time evolution of the temperature of the clast, at a distance $x = 2.6$ mm from the PT vein center and for different distances r from the center of the clast. Although in the reference case a clast of radius 0.75 mm is assimilated by the PT vein (see Fig. 4), in the present case it survives (see Fig. 7).

This simple example raises the question as to whether the power-law distribution I found for the surviving clasts size (see Frequency Distribution of the Surviving Clasts) is dependent on the particular set of parameters. To solve this problem, I have considered another, rather different configuration, in which I simultaneously enlarge the size of the PT vein (now $w = 10$ mm) and the initial radius of the clast (now $r_{\text{cl}} = 4$ mm) and increase the melting temperature of the PT vein (now $T_{\text{melt}} = 1500$°C). I perform nearly 450 additional simulations to build another phase diagram; then I extract the statistics of the surviving clasts, still based on equations (16) and (17). The results are reported as triangles in Figure 6. As expected, the total, cumulative number of clasts, even of small radius, is larger in this case; this is basically due to the effect just discussed in the comparison between Figures 4 and 7 and to the larger size of the PT vein in the present case. Remarkably, this configuration also shows a power-law distribution; there is a higher (negative) slope for larger clasts, as observed in the reference case (circles). The majority of the clast size distribution follows a power law, with an exponent $D = 0.90$, exactly as in the reference case.

Discussion

As with every model of a natural phenomenon, here I make some assumptions. First, I neglect possible spatial heterogeneities in the size of the PT vein, $2w$. Tribological surfaces can deviate from a plane (e.g., Power and Tullis, 1991; Scholz, 2002), and the fault core can be spatially variable, even within the same fault structure (Kirkpatrick and Shipton, 2009; Rathbun and Marone, 2010). Büttner *et al.* (2013) report a high variability in the thickness of the PT veins, ranging from 1 mm to 40 cm; consequently, I can expect that, in general, the PT vein can have nonplanar boundaries. This, in turn, will insert additional spatial dependencies in the Fourier heat conduction equation and in the initial distribution of the temperature $T_0(x)$, making the problem three dimensional instead of one dimensional, as assumed here. Unfortunately, I do not presently have an exact mathematical model, constrained by geological observations, able to describe the spatial heterogeneities of the PT vein in all dimensions. Therefore, my solution in equation (3) should be regarded as an average value (over the depth and the strike direction) of the temperature inside the PT vein.

Second, I assume that the clasts are already present at $t = 0$. As thoroughly discussed by Kirkpatrick and Rowe (2013), many different phenomena can lead to the generation and modifications of clasts during cosesimic slip. In my

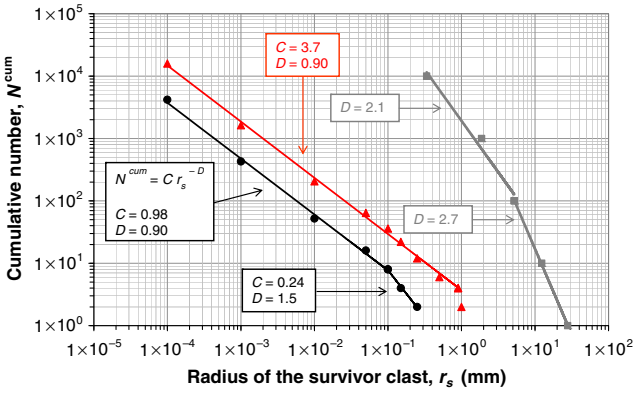

Figure 6. Distribution of the survivor clasts. The ordinate reports the cumulative number of the survivor clasts having a given radius r_s (computed using equation 17). Circles refer to the model parameters listed in Table 1, whereas triangles refer to a modified configuration in which $w = 10$ mm, $r_{cl} = 4$ mm, and $T_{melt} = 1500$°C. For comparison, data from the products of the postmelting clasts of Ray (2004; his table 1b) are also plotted as full gray squares. In all cases, the power-law fitting lines (as from equation 18) are also superimposed. The color version of this figure is available only in the electronic edition.

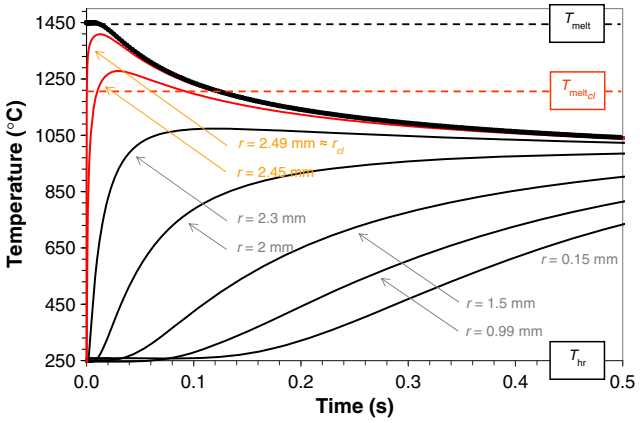

Figure 7. The same as in Figure 4 but with clast radius of 2.5 mm. The color version of this figure is available only in the electronic edition.

idealized picture, I imagine having a snapshot just after the formations of the clasts and ignoring the generation of the PT vein. Moreover, during the generation of the PT vein, I can also observe the injection of some molten materials (at mm to cm scale; e.g., Büttner *et al.*, 2013) into the surrounding damage zone, as a consequence of microscale or mesoscale tension fractures. All these mechanisms are likely to occur during the coseismic time window. At a fundamental level, I consider healing processes that take place locally or that the coseismic slip has just completed, so that the PT vein has been formed (due to frictional heat), clasts have been generated, and possible ejections of melts have been already accomplished. Then, I follow the evolution of the system, starting from that time and from these conditions.

Third, I assume that the PT temperature T is not affected by the presence of the clasts. This assumption is clearly correct when I focus on the temperature of single, isolated clast embedded within the vein; indeed, the volume of a single clast is always smaller than the total volume of the PT vein. The complete treatment of multiple clasts reflects into a multibodies problem, which cannot be easily addressed. When multiple clasts are considered simultaneously in the PT vein, the total volume of all clasts may not be a small fraction of the whole volume of the vein itself. In such a situation, the PT temperature T expressed by equation (3) is not strictly valid; the colder, total volume of the clasts ensemble would decrease the PT temperature faster than the temporal evolution predicted by equation (3). As a consequence, equation (3) should be regarded as an upper bound of the true temperature of the PT vein. On the other hand, the surface temperature of a clast will be lower; this finally translates into the fact that, at a given distance, larger clasts will survive. It is impossible to exactly predict how the statistics of the survived clasts will be affected in this case. However, it is important to remark that, given this model assumption, the computations presented and discussed in the present paper are in general agreement with the observations.

Fourth, in order to have exact solutions (i.e., closed-form analytical solutions) the present treatment assumes that the clasts can be approximated by spheres (see Fig. 1). This assumption is conservative and reasonable for two reasons. First, it is known that survivor clasts also can be affected by plastic deformations, which can elongate them (e.g., Kirkpatrick and Rowe, 2013). However, I do not presently have enough information to be able to select a specific initial shape of the clasts, and I also ignore the exact details of the mechanics of the these plastic deformations; the present choice of an initial spherical shape can be therefore regarded as a conservative choice. Second, data from exhumed samples indicate that from 35% to 90% of the clasts embedded into melted–originated PT veins have roundness greater than 0.4 (Lin, 1999), and Sibson (1975) and Lin (1999) suggest that the rounding of clasts in PT veins is a typical consequence of the occurrence of melting processes within the PT vein. If I hypothesize that a clast (originally having an arbitrary shape) experienced a partial melting (and thus a partial rounding, in agreement with the evidence mentioned above) during a previous coseismic slip episode, then, when I consider the actual slip episode (which can potentially lead to a more complete melting), the initial spherical shape therefore appears as a reasonable assumption.

Finally, because I neglect the latent heat of fusion during the partial melting of a clast (the Stefan problem), equation (14) is intended to be an upper bound of the temperature of the clast after its possible partial melting.

Conclusive Remarks

The main aim of the present study is to understand the destiny of a clast already present and embedded into a molten and just-formed PT vein. PTs are known to be created (and

even destroyed) during coseismic slip failures, as discussed, for example, by Kirkpatrick and Rowe (2013). The occurrence of melting has been investigated theoretically in many studies (e.g., Fialko and Khazan, 2005; Bizzarri and Cocco, 2006b; Nielsen *et al.*, 2008; Bizzarri, 2011, and references cited therein), which indicate that melting at microasperity contacts can often occur. On the other hand, clast formation is due to wear processes (e.g., Sibson, 2003). Remarkably, survivor clasts can be used to retrieve the energy required to create new fracture surfaces (Pittarello *et al.*, 2008), which in turn is of pivotal importance in the formulation of the energy balance for a seismic event.

Starting from the standard formulations in Carslaw and Jaeger (1959), I analytically (and in a closed form) solve the Fourier heat conduction equation, specialized for a PT vein surrounded by a colder host rock. The PT vein is just formed, so that its temperature equals T_{melt}, which exceeds that of the neighboring undamaged rocks. My solution in equation (3) expresses the spatiotemporal evolution of the temperature T inside the PT vein and in the damaged rock (see Figs. 2 and 3). I then found an analytical solution for the temperature within a clast, embedded into the PT vein, which has the surface temperature equal to T. My equation (14) expresses the temperature T_{cl} as a function of the distance x from the PT vein center and of the distance r from the center of the spherical clast (see Fig. 1).

Indeed, the concurrent modeling of (1) the PT and clasts generation through coseismic slip, (2) the possible ejections from the PT vein of molten materials, and (3) the consequent cooling of the whole system is a very complicated phenomenon. Unfortunately, no comprehensive models exist at the moment, and there is insufficient data available to allow us to build a realistic and well-constrained mathematical model. In the present study, I present a first-order approximation of such a complicated situation.

Given the limitations scrutinized in the Discussion section, the theoretical framework proposed here (namely, equations 3 and 14) is, to date, the first model that enables us to theoretically predict the existence of survivor clasts of a given dimension within the molten PT vein. By performing more than 600 numerical experiments with different sets of parameters, I demonstrate that the distance from the PT vein center influences the existence of survivor clasts. Moreover, the temperature distribution inside the clast is not uniform, as physically expected, but it strongly depends on the distance from the center of the clast (see Fig. 4) and on its initial size (Figs. 4 and 7). The evolution of T_{cl} provides us with the maximum size of a clast surviving into the PT vein, at a given distance x from its center.

Moreover, I found that no clasts can be preserved in the inner part of the PT vein for the adopted parameters. Such a strong statement should not be taken too literally; indeed, as stated above, if I consider multiple clasts concurrently heated in the PT vein, their actual surface temperature will be lower than that expressed by equation (3), so some clasts can survive in the PT center or in its proximity. Pittarello *et al.* (2008) found that some clasts survive in the central zone of the PT vein, but these clasts were exclusively of quartz, which has a melting temperature of about 1700°C (e.g., Spray, 2010). (The melting temperature of the clasts assumed in the present model is 1200°C, which is the melting temperature of the plagioclase.) Of course, if I assume that some clasts are composed of quartz, then my model will predict the survival of clasts even in the center of the PT vein, in that the maximum temperature within the PT vein itself is 1450°C. Alternatively, I can also speculate about the possibility that some clasts were originally surrounded by microlites (crystals that grow in and from the PTs melt), which can act as a protection against clast melting, as well as a possible small circulation of clasts, due to postseismic arrangements of the PT vein and of the surrounding rocks. In conclusion, I can interpret my results as a tendency that clasts are preferentially melted in the center of the PT vein compared with the edges.

It also should be noted that some compositional variations of the molten material would be expected at the local scale, where the clasts are completely assimilated into the matrix (e.g., Büttner *et al.*, 2013). The mineral composition of the survivor clasts is used to constrain the (upper) temperature within the PT vein (e.g., Nestola *et al.*, 2010). In this light, the results presented here are a further corroboration of such an interpretation.

In general, the threshold distance x for melting and the maximum size of the survived clasts depend on the adopted parameters, with a pronounced dependence on the size of the PT vein and on the initial radius of the clasts. Clasts with small initial radius have a greater tendency to melt (i.e., a smaller survivability potential) compared with larger clasts, for a given location inside the PT vein. Indeed, I found that the distribution of the surviving clasts follows a power-law relation in terms of their radius (see equation 17 and Fig. 6), regardless of the adopted configuration. This theoretical result is in general agreement with previous microstructural analyses conducted on laboratory and on exhumed samples (Shimamoto and Nagahama, 1992; Ray, 1999, 2004; Pittarello *et al.*, 2008; Kirkpatrick and Rowe, 2013).

Cataclastic fault rocks usually follow a power-law distribution (e.g., Sammis and King, 2007), so it is possible that the distribution of the (survived) clasts into the PT vein somehow reflect their initial distribution (Ray, 2004; Kirkpatrick and Rowe, 2013). In the present paper, I focus on the evolved (by melting process) clast size distribution patterns, rather than on the inherited (by cataclasis) pattern. (As stated in the Frequency Distribution of the Surviving Clasts section, I do not consider any parental clast distribution.) From contemplating the full circles and full triangles in Figure 6, one can see a power-law distribution for both sets of the parameters considered, and this behavior does not depend on the initial size of the clasts. In the framework of the present model, the power-law exponent is different for small and large clasts, in agreement with the conclusions of Ray (2004) and Pittarello *et al.* (2008). Notably, Pittarello *et al.* (2008)

obtain D between 0.2 and 1 for clast dimensions of 2×10^{-5} mm $< r_{cl} < 1 \times 10^{-3}$ mm, which is compatible with my estimate of 0.9 (see Fig. 6). The slope is different for larger dimensions; this is imputable to the assumptions of the present model.

More complicated configurations, also including some spatial heterogeneities in the distribution of the thermal parameters, can be tackled numerically and/or further complicating the partial differential equations to be solved, but, given the assumptions made here, the present results provide a first-order attempt to build a theoretical framework to predict the destiny of a clast within a PT vein.

Data and Resources

All data sources were taken from published works listed in the References.

Acknowledgments

I wish to acknowledge two anonymous reviewers and Associate Editor L. A. Dalguer for useful comments that contributed to improving the manuscript.

References

Andersen, T. B., and H. Austrheim (2006). Fossil earthquakes recorded by pseudotachylytes in mantle peridotite from the Alpine subduction complex of Corsica, *Earth Planet. Sci. Lett.* **242,** 58–72.

Bizzarri, A. (2009). Can flash heating of asperity contacts prevent melting? *Geophys. Res. Lett.* **36,** L11304, doi: 10.1029/2009GL037335.

Bizzarri, A. (2011). Dynamic seismic ruptures on melting fault zones, *J. Geophys. Res.* **116,** no. B02310, doi: 10.1029/2010JB007724.

Bizzarri, A. (2013). Energy flux of propagating ruptures with cohesive force, *Bull. Seismol. Soc. Am.* **103,** no. 5, 2670–2679, doi: 10.1785/0120120335.

Bizzarri, A., and M. Cocco (2006a). A thermal pressurization model for the spontaneous dynamic rupture propagation on a three-dimensional fault: 1. Methodological approach, *J. Geophys. Res.* **111,** no. B05303, doi: 10.1029/2005JB003862.

Bizzarri, A., and M. Cocco (2006b). A thermal pressurization model for the spontaneous dynamic rupture propagation on a three-dimensional fault: 2. Traction evolution and dynamic parameters, *J. Geophys. Res.* **111,** no. B05304, doi: 10.1029/2005JB003864.

Büttner, S. H., S. Sherlock, L. Fryer, J. Lodge, T. Diale, R. Kazondunge, and P. Macey (2013). Controls of host rock mineralogy and H_2O content on the nature of pseudotachylyte melts: Evidence from pan-African faulting in the foreland of the Gariep belt, South Africa, *Tectonophysics* **608,** 552–575.

Carslaw, H. S., and J. C. Jaeger (1959). *Conduction of Heat in Solids*, Oxford University Press, New York, 510 pp.

Chester, J. S., F. M. Chester, and A. K. Kronenberg (2005). Fracture surface energy of the Punchbowl fault, San Andreas system, *Nature* **437,** 133–136, doi: 10.1038/nature03942.

Cocco, M., E. Tinti, and P. Spudich (2007). On the mechanical work absorbed on faults during earthquake ruptures, in *Radiated Energy and the Physics of Earthquakes Faulting*, R. E. Abercrombie, A. McGarr, G. Di Toro, and H. Kanamori (Editors), American Geophysical Monograph, Vol. 170, 237–254, doi: 10.1029/170GM24.

Cowan, D. S. (1999). Do faults preserve a record of seismic slip? A field geologist's opinion, *J. Struct. Geol.* **21,** 995–1001.

Dahlen, F. A. (1977). The balance of energy in earthquake faulting, *Geophys. J. Roy. Astron. Soc.* **48,** 239–261.

Di Toro, G., and G. Pennacchioni (2004). Superheated friction-induced melts in zoned pseudotachylytes within the Adamello tonalites (Italian southern Alps), *J. Struct. Geol.* **26,** 1783–1801.

Di Toro, G., S. Nielsen, and G. Pennacchioni (2005). Earthquake rupture dynamics frozen in exhumed ancient faults, *Nature* **436,** 1009–1012, doi: 10.1038/nature03910.

Fialko, Y. (2004). Temperature fields generated by the elastodynamic propagation of shear cracks in the Earth, *J. Geophys. Res.* **109,** no. B01303, doi: 10.1029/2003JB002497.

Fialko, Y., and Y. Khazan (2005). Fusion by the earthquake fault friction: Stick or slip? *J. Geophys. Res.* **110,** no. B12407, doi: 10.1029/2005JB003869.

Husseini, M. I. (1977). Energy balance for motion along a fault, *Geophys. J. Roy. Astron. Soc.* **49,** 699–714.

Ikesawa, E., A. Sakaguchi, and G. Kimura (2003). Pseudotachylyte from an ancient accretionary complex: Evidence for melt generation during seismic slip along a master décollement? *Geology* **31,** no. 7, 637–640.

Jeffreys, H. (1942). On the mechanics of faulting, *Geol. Mag.* **79,** 291–295, doi: 10.1017/S0016756800076019.

Keulen, N., R. Heilbronner, H. Stünitz, A.-M. Boullier, and H. Ito (2007). Grain size distributions of fault rocks: A comparison between experimentally and naturally deformed granitoids, *J. Struct. Geol.* **29,** no. 8, doi: 10.1016/j.jsg.2007.04.003.

Kirkpatrick, J. D., and C. D. Rowe (2013). Disappearing ink: How pseudotachylytes are lost from the rock record, *J. Struct. Geol.* **52,** 183–198, doi: 10.1016/j.jsg.2013.03.003.

Kirkpatrick, J. D., and Z. K. Shipton (2009). Geologic evidence for multiple slip weakening mechanisms during seismic slip in crystalline rock, *J. Geophys. Res.* **114,** no. B12401, doi: 10.1029/2008JB006037.

Kirkpatrick, J. D., K. J. Dobson, D. F. Mark, Z. K. Shipton, E. E. Brodsky, and F. M. Stuart (2012). The depth of pseudotachylyte formation from detailed thermochronology and constraints on coseismic stress drop variability, *J. Geophys. Res.* **117,** doi: 10.1029/2011JB008846.

Kirkpatrick, J. D., Z. K. Shipton, and C. Persano (2009). Pseudotachylytes: Rarely generated, rarely preserved, or rarely reported? *Bull. Seismol. Soc. Am.* **99,** doi: 10.1785/0120080114.

Kostrov, B. V., and S. Das (1988). *Principles of Earthquake Source Mechanics*, Cambridge University Press, Cambridge, New York.

Lin, A. (1991). Origin of fault-generated pseudotachylytes, *Ph.D. thesis*, The University of Tokyo.

Lin, A. (1999). Roundness of clasts in pseudotachylytes and cataclastic rocks as an indicator of frictional melting, *J. Struct. Geol.* **21,** 473–478.

Lin, A. (2008). Fossil earthquakes: The formation and preservation of pseudotachylytes, *Lecture Notes in Earth Sciences*, Vol. 111, Springer-Verlag, Berlin, Germany, 348 pp.

Maddock, R. H. (1983). Melt origin of fault-generated pseudotachylytes demonstrated by textures, *Geology* **11,** 105–108.

Magloughlin, J. F. (1992). Microstructural and chemical changes associated with cataclasis and frictional melting at shallow crustal levels: The cataclasite–pseudotachylyte connection, *Tectonophysics* **204,** 243–260.

McKenzie, D., and J. Brune (1972). Melting on fault planes during large earthquakes, *Geophys. J. Roy. Astron. Soc.* **29,** 65–78.

Nestola, F., S. Mittempergher, and G. Di Toro (2010). Evidence of dmisteinbergite (hexagonal form of $CaAl_2Si_2O_8$) in pseudotachylyte: A tool to constrain the thermal history of a seismic event, *Am. Mineral.* **95,** nos. 2/3, 405–409, doi: 10.2138/am.2010.3393.

Nielsen, S., G. Di Toro, T. Hirose, and T. Shimamoto (2008). Frictional melt and seismic slip, *J. Geophys. Res.* **113,** no. B01308, doi: 10.1029/2007JB005122.

Ohtomo, Y., and T. Shimamoto (1994). Significance of thermal fracturing in the generation of fault gouge during rapid fault motion: An experimental verification, *Struct. Geol.* **39,** 35–44 (in Japanese with English abstract).

Philpotts, A. R. (1964). Origin of pseudotachylytes, *Am. J. Sci.* **262,** 1008–1035.

Piessens, R., E. deDoncker–Kapenga, C. W. Uberhuber, and D. K. Kahaner (1983). *QUADPACK*, Springer-Verlag, New York.

Pittarello, L., and C. Koeberl (2013). Clast size distribution and quantitative petrography of shocked and unshocked rocks from the El'gygytgyn impact structure, *Meteoritics Planet. Sci.* **48,** no. 7, 1325–1338, doi: 10.1111/maps.12070.

Pittarello, L., G. Di Toro, A. Bizzarri, G. Pennacchioni, J. Hadizadeh, and M. Cocco (2008). Energy partitioning during seismic slip in pseudotachylyte-bearing faults (Gole Larghe fault, Adamello, Italy), *Earth Planet. Sci. Lett.* **269,** 131–139, doi: 10.1016/j.epsl.2008.01.052.

Power, W. L., and T. E. Tullis (1991). Euclidean and fractal models for the description of rock surface roughness, *J. Geophys. Res.* **96,** 415–424, doi: 10.1029/90JB02107.

Rabinowicz, E. (1965). *Friction and Wear of Materials*, John Wiley, New York.

Rathbun, A. P., and C. J. Marone (2010). Effect of strain localization on frictional behavior of sheared granular materials, *J. Geophys. Res.* **115,** no. B01204, doi: 10.1029/2009JB006466.

Ray, S. K. (1999). Transformation of cataclastically deformed rocks to pseudotachylyte by pervasion of frictional melt: Inferences from clast–size analysis, *Tectonophysics* **301,** 283–304.

Ray, S. K. (2004). Melt–clast interaction and power-law size distribution of clasts in pseudotachylytes, *J. Struct. Geol.* **26,** 1831–1843, doi: 10.1016/j.jsg.2004.02.009.

Reches, Z., and T. A. Dewers (2005). Gouge formation by dynamic pulverization during earthquake rupture, *Earth Planet. Sci. Lett.* **235,** 361–374.

Rempel, A. W., and J. R. Rice (2006). Thermal pressurization and onset of melting in fault zones, *J. Geophys. Res.* **111,** no. B09314, doi: 10.1029/2006JB004314.

Rivera, L., and H. Kanamori (2005). Representation of the radiated energy in earthquakes, *Geophys. J. Int.* **162,** 148–155, doi: 10.1111/j.1365-246X.2005.02648.x.

Rowe, C. D., J. C. Moore, F. Meneghini, and A. W. McKiernan (2005). Large-scale pseudotachylytes and fluidized cataclasites from an ancient subduction thrust fault, *Geology* **33,** 937–940.

Rudnicki, J. W., and L. B. Freund (1981). On energy radiation from seismic sources, *Bull. Seismol. Soc. Am.* **71,** 583–595.

Sammis, C. G., and G. C. P. King (2007). Mechanical origin of power law scaling in fault zone rock, *Geophys. Res. Lett.* **34,** L04312, doi: 10.1029/2006GL028548.

Scholz, C. H. (2002). *The Mechanics of Earthquakes and Faulting*, Second Ed., Cambridge University Press, New York, 439 pp.

Shand, S. J. (1916). The pseudotachylyte of Parijs (Orange Free State) and its relation to "trap-shotten gneiss" and "flinty crush rock," *Q. J. Geol. Soc. Lond.* **72,** 198–221.

Shimamoto, T., and H. Nagahama (1992). An argument against a crush origin for pseudotachylytes based on the analysis of clast-size distribution, *J. Struct. Geol.* **14,** 999–1006.

Sibson, R. H. (1975). Generation of pseudotachylyte by ancient seismic faulting, *Geophys. J. Roy. Astron. Soc.* **43,** 775–794.

Sibson, R. H. (2003). Thickness of the seismic slip zone, *Bull. Seismol. Soc. Am.* **93,** no. 3, 1169–1178.

Sibson, R. H., and V. G. Toy (2006). The habitat of fault-generated pseudotachylyte: Presence vs. absence of friction-melt, in earthquakes, in *Radiated Energy and the Physics of Faulting*, R. E. Abercrombie, A. McGarr, G. Di Toro, and H. Kanamori (Editors), American Geophysical Monograph, Vol. 170, 153–166.

Spray, J. G. (1987). Artificial generation of pseudotachylyte using friction welding apparatus, *Contrib. Mineral. Petrol.* **99,** 464–475.

Spray, J. G. (1992). A physical basis for the frictional melting of some rock-forming minerals, *Tectonophysics* **204,** 205–221.

Spray, J. G. (1993). Viscosity determinations of some frictionally generated silicate melts: Implications for fault zone rheology at high strain rates, *J. Geophys. Res.* **98,** 8053–8068.

Spray, J. G. (1995). Pseudotachylyte controversy: Fact or friction? *Geology* **23,** 1119–1122.

Spray, J. G. (2010). Frictional melting processes in planetary materials: From hypervelocity impact to earthquakes, *Ann. Rev. Earth Planet. Sci.* **28,** 221–254.

Storti, F., F. Rossetti, and F. Salvini (2001). Structural architecture and displacement accommodation mechanisms at the termination of the Priestley Fault, northern Victoria Land, Antarctica, *Tectonophysics* **341,** 141–161.

Tsutsumi, A. (1999). Size distribution of clasts in experimentally produced pseudotachylytes, *J. Struct. Geol.* **21,** 305–312.

Ujiie, K., H. Yamaguchi, A. Sakaguchi, and S. Toh, (2007). Pseudotachylytes in an ancient accretionary complex and implications for melt lubrication during subduction zone earthquakes, *J. Struct. Geol.* **29,** 599–613.

Appendix A

Estimation of the Surface Temperature of the Clast

One essential ingredient to determine the temperature inside a clast, $T_{\rm cl}(r,t;x)$, is its surface temperature. In the Temperature Inside a Single Clast section, equations (6)–(8) express this temperature by assuming the surface temperature of the spherical clast is spatially uniform and equal to $T(x,t)$, that is, equal to the temperature at the location of the clast center (see Fig. 1). Such a temperature is maximum at $x-r_{\rm cl}$ and minimum at $x+r_{\rm cl}$ (which represent the minimum and the maximum distance, respectively, from the pseudotachylyte [PT] vein center, $x=0$). At a given time t, $T(x,t)$ is intermediate between $T(x+r_{\rm cl},t)$ and $T(x-r_{\rm cl},t)$; that is, $T(x+r_{\rm cl},t)<T(x,t)<T(x-r_{\rm cl},t)$.

Obviously, if $r_{\rm cl}$ is small (formally, if the condition $r_{\rm cl}\ll w$ is met), the temperature difference between the two above-mentioned end points is negligible, so that $T(x,t)$ can be safely taken as the representative surface temperature of the whole clast.

In general, I can define the average surface temperature of the clast as

$$\langle T\rangle=\frac{1}{4\pi r_{\rm cl}^2}\int_{\Sigma_{r_{\rm cl}}} T\,d\sigma; \tag{A1}$$

that is, the temperature is averaged over its spherical surface. In equation (A1) $\Sigma_{r_{\rm cl}}$ is the boundary of the sphere of radius $r_{\rm cl}$ (i.e., its surface) and $d\sigma$ is the differential. In polar coordinates, I have

$$\begin{cases} x=x_0+r_{\rm cl}\sin\theta\cos\varphi \\ y=y_0+r_{\rm cl}\sin\theta\sin\varphi \\ z=z_0+r_{\rm cl}\cos\theta \end{cases}, \tag{A2}$$

in which $\theta\in[0,\pi]$, $\varphi\in[0,2\pi]$, and (x_0,y_0,z_0) is the position in $\mathbb{R}^3$ of the center of the clast. Considering that T does not depend on y_0 and z_0 and that $d\sigma=r_{\rm cl}^2\sin\theta\,d\theta\,d\varphi$, I can write equation (A1) as

$$\langle T\rangle=\frac{1}{4\pi r_{\rm cl}^2}\int_0^{2\pi}d\varphi\int_0^{\pi}d\theta\,T(x_0+r_{\rm cl}\sin\theta\cos\phi,t)r_{\rm cl}^2\sin\theta. \tag{A3}$$

Now, I consider the McLaurin series expansion of the (regular) function T at first order, which is

$$T(x_0 + r_{\mathrm{cl}} \sin\theta \cos\varphi, t) \approx T(x_0, t) + \frac{\partial T}{\partial x}|_{x_0} r_{\mathrm{cl}} \sin\theta \cos\varphi, \tag{A4}$$

and rewrite equation (A3) as

$$\begin{aligned}\langle T \rangle &\approx \frac{1}{4\pi}\left(\int_0^{2\pi} d\varphi \int_0^{\pi} d\theta\, T(x_0, t) \sin\theta \right.\\ &\quad \left. + \int_0^{2\pi} d\varphi \int_0^{\pi} d\theta \frac{\partial T}{\partial x}|_{x_0} r_{\mathrm{cl}} \sin\theta \cos\varphi\right)\\ &= \frac{1}{4\pi}\left(T(x_0, t) \int_0^{2\pi} d\varphi \int_0^{\pi} d\theta \sin\theta \right.\\ &\quad \left. + r_{\mathrm{cl}} \frac{\partial T}{\partial x}|_{x_0} \int_0^{2\pi} d\varphi \int_0^{\pi} d\theta \sin\theta \cos\varphi\right).\end{aligned}$$

Because

$$\int_0^{2\pi} d\varphi \int_0^{\pi} d\theta \sin\theta = 4\pi \quad \text{and}$$
$$\int_0^{2\pi} d\varphi \int_0^{\pi} d\theta \sin\theta \cos\varphi = 0,$$

I simply obtain

$$\langle T \rangle \approx T(x_0, t). \tag{A6}$$

In words, equation (A6) states that the average surface temperature of a clast can be approximated, at first-order series expansion, as the temperature T at the distance x_0 of its center from the center of the PT vein. Therefore, equation (A6) mathematically demonstrates that the combination of equations (6) and (8) is valid to estimate the temperature of a clast subject to the temperature field T, given in turn by equation (3).

Istituto Nazionale di Geofisica e Vulcanologia
Sezione di Bologna
Via Donato Creti, 12
40128 Bologna, Italy
andrea.bizzarri@ingv.it

Manuscript received 26 March 2014;
Published Online 19 August 2014